ACCOUNTS
of chemical research

# Photoactive Ruthenium Nitrosyls as NO Donors: How To Sensitize Them toward Visible Light

NICOLE L. FRY AND PRADIP K. MASCHARAK*

*Department of Chemistry and Biochemistry, University of California, Santa Cruz, California 95064, United States*

RECEIVED ON DECEMBER 2, 2010

## CONSPECTUS

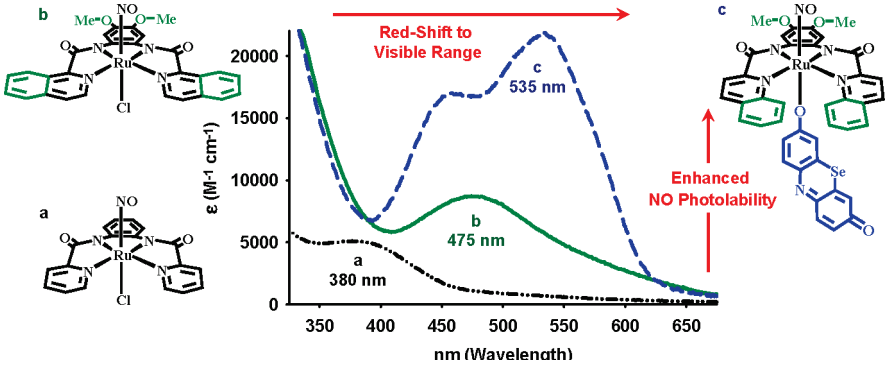


Nitric oxide (NO) can induce apoptosis (programmed cell death) at micromolar or higher doses. Although cell death via NO-induced apoptosis has been studied quite extensively, the targeted delivery of such doses of NO to infected or malignant tissues has not been achieved. The primary obstacle is indiscriminate NO release from typical systemic donors such as glycerin trinitrate: once administered, the drug travels throughout the body, and NO is released through a variety of enzymatic, redox, and pH-dependent pathways.

Photosensitive NO donors have the ability to surmount this difficulty through the use of light as a localized stimulus for NO delivery. The potential of the method has prompted synthetic research efforts toward new NO donors for use as photopharmaceuticals in the treatment of infections and malignancies. Over the past few years, we have designed and synthesized several metal nitrosyls (NO complexes of metals) that rapidly release NO when exposed to low-power (milliwatt or greater) light of various wavelengths. Among them, the ruthenium nitrosyls exhibit exceptional stability in biological media. However, typical ruthenium nitrosyls release NO upon exposure to UV light, which is hardly suitable for phototherapy. By following a few novel synthetic strategies, we have overcome this problem and synthesized a variety of ruthenium nitrosyls that strongly absorb light in the 400−600-nm range and rapidly release NO under such illumination. In this Account, we describe our progress in designing photoactive ruthenium nitrosyls as visible-light-sensitive NO donors.

Our research has shown that alteration of the ligands, in terms of (i) donor atoms, (ii) extent of conjugation, and (iii) substituents on the ligand frames, sensitizes the final ruthenium nitrosyls toward visible light in a predictable fashion. Density functional theory (DFT) and time-dependent DFT (TDDFT) calculations provide guidance in this "smart design" of ligands. We have also demonstrated that direct attachment of dye molecules as light-harvesting antennas also sensitize ruthenium nitrosyls to visible light, and TDDFT calculations provide insight into the mechanisms of sensitization by this technique. The fluorescence of the dye ligands makes these NO donors "trackable" within cellular matrices. Selected ruthenium nitrosyls have been used to deliver NO to cellular targets to induce apoptosis. Our open-design strategies allow the isolation of a variety of these ruthenium nitrosyls, depending on the choices of the ligand frames and dyes. These designed nitrosyls will thus be valuable in the future endeavor of synthesizing novel pharmaceuticals for phototherapy.

## Introduction

During the past three decades, the discovery of the various physiological and pathological roles of nitric oxide (NO)[1−4] has spurred intense research interest in the design and isolation of exogenous NO donors that can be used for blood pressure control (in treatment of angina pectoris),[1,5]

Published on the Web 03/01/2011 www.pubs.acs.org/accounts
10.1021/ar100155t 

modulation of platelet adhesion activity on surgical equipment and stents,[6,7] antimicrobial applications (to reduce bacterial and parasitic loads),[8,9] and destruction of malignant locales via NO-induced apoptosis.[10−12] One typical problem associated with typical systemic NO donors such as glyceryl trinitrate, *S*-nitrosothiols, and diazeniumdiolates (NONOates) lies in the lack of control for site-specific NO delivery. Once administered, the drug goes everywhere in the body, and NO is released via a variety of enzymatic, redox, or pH-dependent pathways. Such inexorability however could be circumvented via their incorporation in biocompatible polymer matrices. Such hybrid materials allow delivery of NO to selected locales with more precision.[13,14] Nevertheless, a better triggering mechanism for NO release from a designed NO donor is highly desirable for site-specific NO delivery in, say, destruction of malignant or infected cellular targets with pathological concentration of NO without severe hypotensive effects elsewhere in the body.

Metal nitrosyls has been investigated for quite sometime as possible NO donors in biological systems.[15−17] Early success in NO delivery by sodium nitroprusside (SNP) stimulated research in this area. Since many metal nitrosyls (including SNP) release NO upon exposure to light, they offer an additional advantage. *Indeed, light is a convenient trigger in the NO delivery process.* The use of typical metal nitrosyls such as SNP however has been somewhat limited because of toxicity related to photoproducts (the remaining metal complexes) or loss of ancillary ligands ($CN^-$ in this case) and stability in biological media. Since ruthenium nitrosyls are quite robust, most of the complications could be avoided.[16] In addition, small quantities of ruthenium complexes are well-tolerated as exemplified by the results of clinical trials of cancer therapy with the Ru-drug NAMI ($[Ru(im)_2Cl_4]^-$, im = imidazole).[18] The photoactivity of ruthenium nitrosyls has been known for over 40 years. For example, in 1971, Cox and Wallace noted that an acidic aqueous solution of $K_2[Ru(Cl)_5(NO)]$ turned brown when exposed to light due to loss of NO, while it was thermally stable in the dark over days.[19] Research during the following decades identified several ruthenium nitrosyls that produce NO upon exposure to light.[16,20,21] However, the majority of these nitrosyls suffer from low quantum yield values ($\phi$) and most importantly their requirement of exposure to high power UV light (300−400 nm) for effective NO release. Such exposure is definitely harmful to tissues. However if new ruthenium nitrosyls that rapidly release NO upon exposure to visible light can be synthesized, they will be very valuable in delivering NO to malignant targets. Such treatment will fall under the topic of photodynamic therapy (PDT).[22,23] An advantage of NO-induced PDT lies in the fact that apoptotic cell death hardly elicits immune response and causes less pain, swelling, and scar tissue formation, all distinct and more desirable outcomes compared with the singlet oxygen-induced cell destruction in conventional PDT with heme-containing sensitizers.

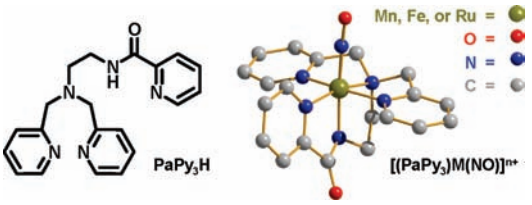


**FIGURE 1.** The pentadentated $PaPy_3H$ ligand (left). Manganese, iron, or ruthenium nitrosyls derived from the deprotonated $PaPy_3^-$ ligand (right).

During the past few years, we have undertaken the task of isolation of designed metal nitrosyls that can be triggered via low-power (watt to milliwatt) light of various wavelengths (400−1000 nm).[24−28] Smart design of polydentate ligands has been a major part of this research. Use of such ligands not only alleviates the problem related to loss of ancillary ligands but also allows one to modulate the sensitivity of the resultant metal nitrosyls toward light of different wavelengths. In this Account, we present the various strategies that we have adopted to synthesize various designed ruthenium nitrosyls that exhibit efficient NO release (moderate to high $\phi$ values) upon illumination to low-power visible lights, that is, light of wavelengths longer than the range required for typical nitrosyls like $[Ru(NH_3)_5(NO)]Cl_3$. The underlying principles leading to sensitization of the ruthenium nitrosyls to visible light are also discussed.

## Alteration of the Ligand Frame

**a. Variation of Donor Groups.** Research in our lab on NO-donating metal nitrosyls began with the synthesis of manganese, iron, and ruthenium nitrosyls derived from the designed polypyridine pentadentate ligand $PaPy_3H$ (*N*,*N*-bis(2-pyridylmethyl)amine-*N*-ethyl-2-pyridine-2-carboxamide; H denotes the dissociable amide H) with a single carboxamido donor, namely, $[(PaPy_3)Mn(NO)](ClO_4)$, $[(PaPy_3)Fe(NO)](ClO_4)_2$, and $[(PaPy_3)Ru(NO)](BF_4)_2$ (Figure 1). Both the manganese[24] and iron[26,27] nitrosyls rapidly release NO upon illumination with 5−10 mW of visible light (500−600 nm). However, both nitrosyls exhibit limited stability in aqueous buffer. The corresponding ruthenium nitrosyl $[(PaPy_3)Ru(NO)](BF_4)_2$ (**1**, the first $\{RuNO\}^6$ nitrosyl[28] in our

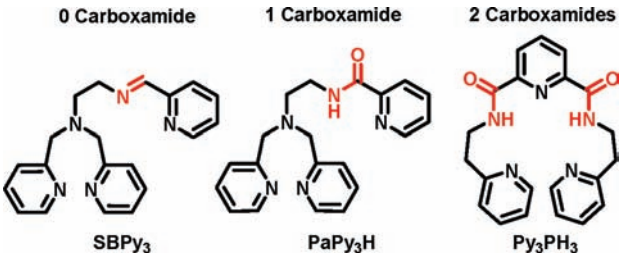


**FIGURE 2.** Pentadentate ligands with zero ($SBPy_3$), one ($PaPy_3H$), and two ($Py_3PH_3$) carboxamide donors.

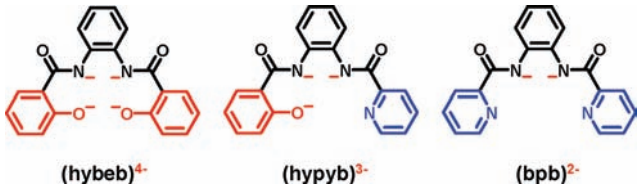


**FIGURE 3.** Dicarboxamide tetradentate ligands of increasing charge ($(bpb)^{2-} < (hypyb)^{3-} < (hybeb)^{4-}$) with phenolato-O or neutral pyridine-N donors.

work)[29] on the other hand is indefinitely stable in biological media and has been employed to deliver NO to such biological targets as cytochrome *c* oxidase[30] and soluble guanylate cyclase.[31] The principal limitation with this NO donor has been its lack of NO photolability under visible light. Clearly, further alteration of the ligand frame was required to overcome this deficiency.

With $[(PaPy_3)Ru(NO)](BF_4)_2$ (**1**) in hand, we first began to examine what features of the polydentate ligand frame contribute to the overall photolability of the $\{RuNO\}^6$ nitrosyl. Most noticeably, the deprotonated carboxamido nitrogen (a strong $\sigma$-donating negatively charged donor) is trans to NO. This feature prompted us to first investigate the role of the carboxamide functionality in the overall NO photolability of the nitrosyls. We therefore synthesized two other $\{RuNO\}^6$ nitrosyls with similar polypyridine pentadentate ligands with zero or two carboxamido-N donor atoms, namely, $[(SBPy_3)Ru(NO)](BF_4)_3$ (**2**, $SBPy_3$ = *N,N*-bis(2-pyridylmethyl)-amine-*N*-ethyl-2-pyridine-2-aldimine) and $[(Py_3P)Ru(NO)]BF_4$ (**3**, $Py_3PH_2$ = *N,N*-bis(2-(2-pyridyl)ethyl)pyridine-2,6-dicarboxamide), respectively.[32] The ligand frame of **2** is similar to that of **1** except for the replacement of the charged carboxamido-N with a neutral imine-N donor atom (Figure 2). Both carboxamido-N and imine-N donors are bound trans to NO in **1** and **2**, respectively. Conversely, **3** contains two carboxamido-N donors in the equatorial plane with a neutral pyridine-N bound trans to NO. Interestingly, as one increases the number of carboxamido-N donors, the absorption bands of the resulting nitrosyls are red-shifted. For example, **2** with Schiff base functionality absorbs at 310 nm, while **1** and **3** (with one and two carboxamido-N donor) absorb at 410 and 530 nm, respectively (all measurements in MeCN). All three nitrosyls show photolability upon exposure to low-power (2−5 mW) UV light. However, only **3** shows appreciable photoactivity when exposed to visible light with a quantum yield at 532 nm ($\phi_{532}$) of 0.050 in MeCN. In addition, the presence of the carboxamide group in such $\{RuNO\}^6$ nitrosyls imparts more stability in aqueous medium. For example, unlike **1** and **3**, **2** shows partial degradation (with concomitant NO → $NO_2$ conversion)[16] in aqueous buffer (pH 7). Thus ligands with carboxamide groups afford $\{RuNO\}^6$ nitrosyls that are more suitable for photoinduced NO delivery to biological targets.

**b. Changes in Donor Atom Set.** In the next phase, we synthesized $\{RuNO\}^6$ nitrosyls derived from several tetradentate ligands with two built-in carboxamide groups along with varying combinations of neutral pyridine-N and charged phenolato-O donor atoms (Figure 3) to elucidate the effects of donor strength on their absorption parameters and quantum yield efficiencies in the visible range. These $\{RuNO\}^6$ nitrosyls, namely, $(NEt_4)_2[(hybeb)Ru(NO)(OEt)]$ (**4**, $H_4$hybeb = 1,2-bis(2-hydroxybenzamido)-benzene), $(PPh_4)$-[(hypyb)Ru(NO)(OEt)] (**5**, $H_3$hypyb =1-(2-hydroxybenzamido)-2-(2-pyridinecarboxamido)benzene), and [(bpb)Ru(NO)(OEt)] (**6**, $H_2$bpb = 1,2-bis(pyridine-2-carboxamido)-benzene) each have the tetradentate ligand frame bound in the equatorial plane with NO and $OEt^-$ bound in their axial positions.[33] The overall negative charge of **4**, **5**, and **6** decreases as the number of negative phenolato-O donors decreases from two to one to zero, respectively. However, the red shift of the absorption band of these nitrosyls follows the order **4** (320 nm) < **6** (380 nm) < **5** (420 nm). A similar trend is seen for the quantum yield values measured at 300 nm: **4** ($\phi = 0.025$), **5** ($\phi = 0.067$), and **6** ($\phi = 0.051$). This trend shows that simple increase in the number of charged donor atoms is *not enough* to enhance the extent of absorption of low-energy (visible) light or the quantum yield efficiency of NO release.

To gain further insight into the roles of specific donor atoms involved in the absorption of lower energy light leading to the photorelease of NO, we have performed density functional theory (DFT) and time-dependent DFT (TDDFT) calculations on **4**−**6**.[33] Previous theoretical studies by Franco and co-workers on simple $\{RuNO\}^6$ nitrosyls, such as $[Ru(NH_3)_5NO]^{3+}$ and $[Ru(NH_3)_4(Cl)NO]^{2+}$, suggest that the photolability of these complexes is initiated by high-energy (330 nm) $d\pi(Ru) \rightarrow \pi^*(NO)$ transitions.[20] However, as the ligand frame becomes more complex, this transition begins to comprise more ligand character. For example, the

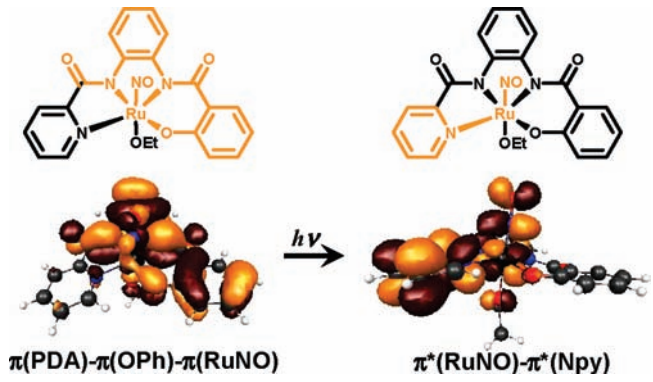


**FIGURE 4.** Molecular orbitals involved in calculated electronic transition responsible for the absorbance band at 420 nm of $(PPh_4)[(hypyb)Ru(NO)(OEt)]$ (**5**). The locations of the molecular orbitals are highlighted in the structure of **5** above.

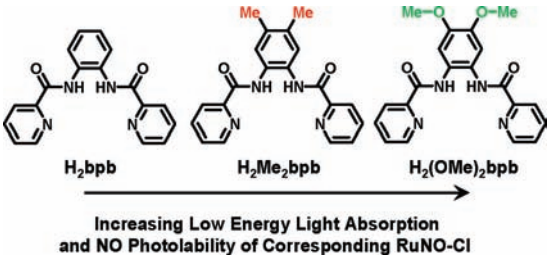


**FIGURE 5.** Dicarboxamide tetradentate ligands with substituents of increasing electron donor strength (H < Me < OMe).

photobands (absorption band associated with NO photolability) of **4**, **5**, and **6** all arise from transitions starting in molecular orbitals (MOs) with partial phenylenedicarboxamide (PDA) character. This explains the experimental data suggesting the importance of carboxamide donors in the enhanced photolability of carboxamide-containing $\{RuNO\}^6$ nitrosyls. Further, the addition of phenolato-O donors in the ligand frame seems to raise the energy of the highest occupied MOs, which are primarily centered on the PDA moiety, the phenolate group (PhO), and the RuNO unit, while addition of pyridine donors lowers the energy of the lowest unoccupied MOs, which contain pyridine (Npy) and RuNO antibonding character. Thus complex **5**, which contains both phenolato and pyridine donors, has the lowest energy transition from an occupied orbital with partial phenolato character ($\pi$(PDA)−$\pi$(PhO)−$\pi$(RuNO)) into an orbital with partial pyridine character ($\pi^*$(RuNO)−$\pi^*$(Npy), Figure 4). In addition, complex **4**, which has all charged (electron-donating) donors and no electron-accepting groups exhibits only high-energy transitions. Thus, it becomes apparent that the correct mix of electron-accepting and electron-donating groups in the ligand frame promotes the absorption of lower energy light (and concomitant NO photolability) in this type of $\{RuNO\}^6$ nitrosyl derived from designed ligands.

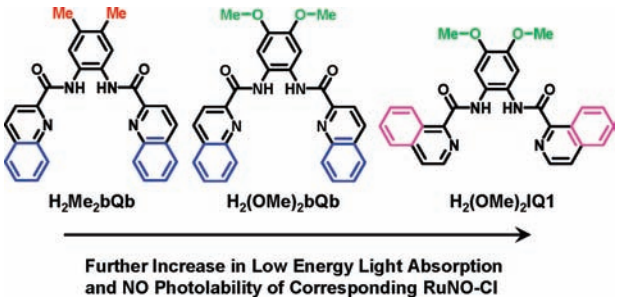


**FIGURE 6.** Dicarboxamide tetradentate ligands with Me or OMe substituents and extended conjugation (quinoline or 1-isoquinoline moieties in place of pyridine).

**c. Addition of Substituents on the Ligand Frame.** Since substitution of the aromatic ring(s) of the ligand frame can alter the electron-donating and accepting capacities of the donor centers, substitution of the tetradentate dicarboxamide $N_4$ ligand frame ($R_2bpb^{2-}$) was attempted in our next phase. Specifically, a series of ruthenium nitrosyls was synthesized with ligands containing electron-donating groups of increasing strength (H, Me, OMe) on the PDA region of the ligand frame (Figure 5), namely, [(bpb)Ru(NO)(Cl)] (**7**),[34] [($Me_2$bpb)Ru(NO)(Cl)] (**8**),[34] and [($(OMe)_2$bpb)Ru(NO)(Cl)] (**9**).[35] The photoband of these $\{RuNO\}^6$ nitrosyls is systematically shifted from 380 to 395 to 420 nm, respectively (see Figure 8). The basis of this phenomenon can be understood with the help of the previously described TDDFT study, in which the photoband of ruthenium nitrosyls with $bpb^{2-}$ type ligand frames was assigned to a $\pi$(PDA)−$\pi$(RuNO) → $\pi^*$(RuNO)$\pi$(Py) transition. Such a transition would indeed require less energy with the addition of electron-donating groups of increasing strength on the PDA moiety. The **7**−**9** set of $\{RuNO\}^6$ nitrosyls clearly demonstrates that the $\pi$(PDA)−$\pi$(RuNO) → $\pi^*$(RuNO)$\pi$(Py) transition can be readily manipulated by appropriate substitution on the ligand frame. In addition, the extinction coefficient ($\varepsilon$) of the photoband also increases significantly when a strongly electron-donating group (like OMe) is added to the PDA moiety. Thus, **9** exhibits an $\varepsilon$ value of 7800 $M^{-1}$ $cm^{-1}$, which is greater than the $\varepsilon$ value of **7** (5100 $M^{-1}$ $cm^{-1}$). And finally, the quantum yield values of NO photorelease at 500 nm ($\phi_{500}$) increase in the order **7** < **8** < **9**.

**d. Extention of Conjugation in the Ligand Frame.** Just as the position of the photoband of the $\{RuNO\}^6$ nitrosyls can be adjusted via substitution, extension of conjugation of the pyridine arms can also lead to a red shift of the photoband and result in enhanced sensitivity to visible light. In our work,

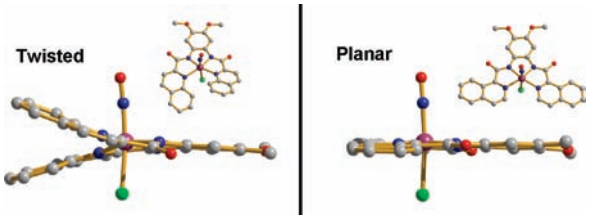


**FIGURE 7.** X-ray structures of [((OMe)$_2$bQb)Ru(NO)(Cl)] (**11**, left) and [((OMe)$_2$IQ1)Ru(NO)(Cl)] (**12**, right), displaying the differing amounts of twist in their in-plane ligand frames.

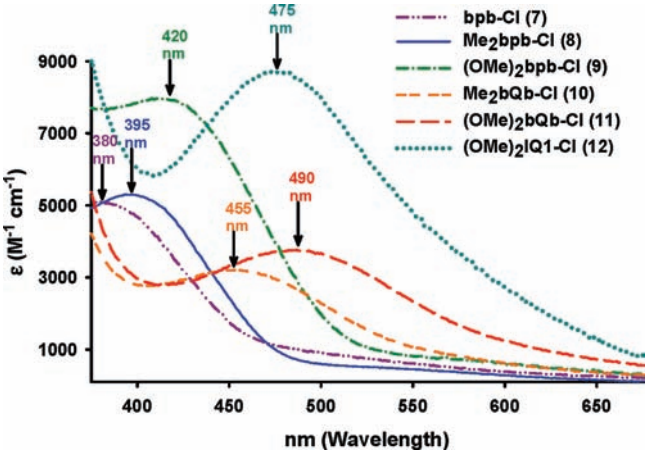


**FIGURE 8.** Electronic absorption spectra of chloride bound $\{RuNO\}^6$ nitrosyls (**7**−**12**) displaying a systematic red shift and increase in $\varepsilon$ values of the photoband as the ligand frame is changed.

we have extended the conjugation through replacement of the pyridine rings with quinolines. Both quinoline (Q) and 1-isoqulinoline (IQ1) were used in the design of the ligand frames (Figure 6) to isolate [(Me$_2$bQb)Ru(NO)(Cl)] (**10**),[34] [((OMe)$_2$bQb)Ru(NO)(Cl)] (**11**),[35] and [((OMe)$_2$IQ1)Ru(NO)(Cl)] (**12**).[35] The addition of Q in [((OMe)$_2$bQb)Ru(NO)(Cl)] (**11**, 490 nm) results in a 70 nm red shift in the absorption maximum ($\lambda_{max}$) of the photoband compared with that of [((OMe)$_2$bpb)Ru(NO)(Cl)] (**9**, 420 nm). With the use of IQ1 in [((OMe)$_2$IQ1)Ru(NO)(Cl)] (**12**, 475 nm), there is a more modest red shift of 55 nm. Interestingly, the extended quinoline (Q) moieties in the ligand frame of **10** and **11** lead to a twisted in-plane ligand structure presumably due to steric interactions between the two quinoline substituents (Figure 7, left panel).[34] However, the use of pyridine (in **7**−**9**) or IQ1 donors (in **12**) relieves such interactions allowing a planar equatorial ligand frame (Figure 7, right panel).[35] When the $\varepsilon$ values of **7**−**12** are compared, another interesting trend becomes evident. As the twist of the bound Q-based ligand frames is relieved and the electron-donating effects of the substituents are increased, the overall $\varepsilon$ values of the photobands of the nitrosyls (in the 350−600 nm region, Figure 8) increase substantially. As a result, **12** not only exhibits the highest $\varepsilon$ values (8700 $M^{-1}$ $cm^{-1}$) but also has the highest $\phi_{500}$ value of 0.035.

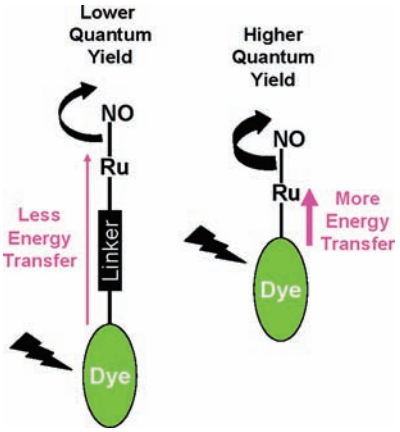


**FIGURE 9.** Ruthenium nitrosyls directly coordinated to a sensitizing dye chromophore (right) have higher quantum yields of NO photorelease than nitorsyls with the dye coordinated through a linker (left).


**FIGURE 10.** Ruthenium nitrosyl−dye conjugates (**12-Resf** shown) with Resf bound trans to NO.

## Direct Attachment of Light-Harvesting Dyes

Although alteration of ligand frames allowed us to achieve good sensitivity of designed $\{RuNO\}^6$ nitrosyls to visible light, their $\phi_{500}$ values of NO photorelease remained somewhat modest, in the range of 0.010−0.050. In an effort to further increase the visible light absorption by our ruthenium nitrosyls and enhance their $\phi_{500}$ values, we adopted a new strategy of direct attachment of dye chromophores (as light-harvesting units) to these nitrosyls and determined their effects on the NO photolability of the resulting nitrosyl−dye conjugates under visible light.[37] Previously, Ford and co-workers have used chromophores like protoporphyrin IX ($\lambda_{max} \approx 400$ nm) and fluorescein ($\lambda_{max} \approx 450$ nm) connected via $(CH_2)_n$ linkers to Roussin's salt esters

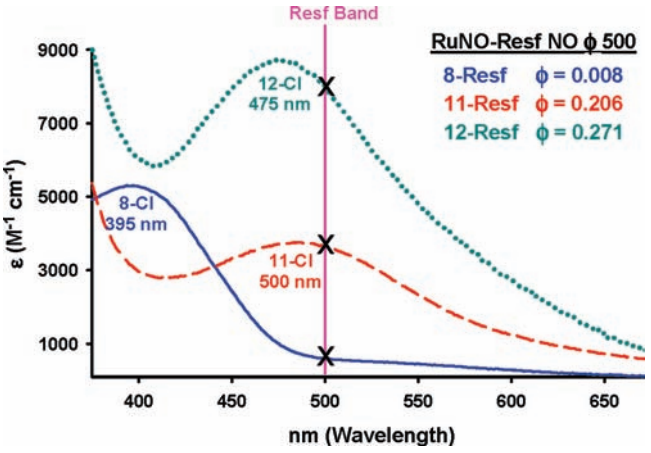


**FIGURE 11.** Electronic absorption spectra of [($Me_2$bpb)Ru(NO)(Cl)] (**8-Cl**), [(($OMe)_2$bQb)Ru(NO)(Cl)] (**11-Cl**), and [(($OMe)_2$IQ1)Ru(NO)(Cl)] (**12-Cl**). Black X's represents points of overlap of RuNO−Cl photoband with the bound Resf absorption band at 500 nm. Larger overlap leads to higher quantum yield values of NO release in the corresponding RuNO−Resf nitrosyls (inset).

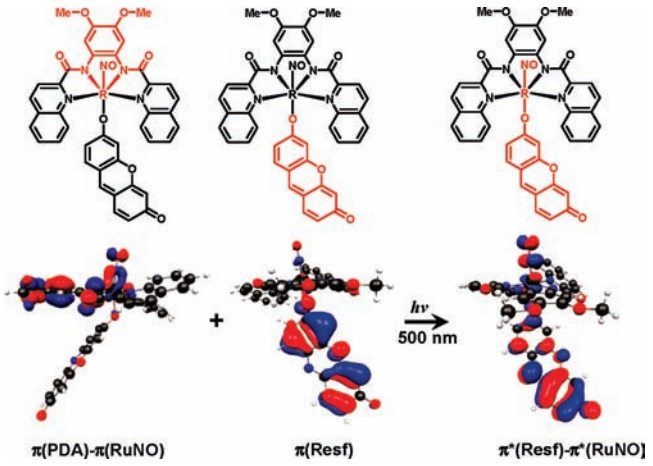


**FIGURE 12.** Molecular orbitals involved in the calculated electronic transition responsible for the absorbance band at 500 nm of [(($OMe)_2$bQb)Ru(NO)(Resf)] (**11-Resf**). The locations of the molecular orbitals are highlighted in the structure of **11-Resf** above.

(generating PPIX-RSE or Fluor-RSE).[38,39] This indirect dye attachment led to moderate improvement in the quantum yield of NO photolability ($\phi$ in the range of 0.00025−0.00052). We decided to improve upon this strategy by *directly conjugating* selected visible light-absorbing chromophores to the RuNO unit to enhance the sensitivity of our ruthenium nitrosyls to visible light (Figure 9).

In our work, we chose the tricyclic phenoxazin dye resorufin (Resf) and synthesized a series of dye−nitrosyl conjugates. In these $\{RuNO\}^6$ nitrosyls with various tetradentate dicarboxamide ligands in the equatorial plane, namely, [($Me_2$bpb)Ru(NO)(Resf)] (**8-Resf**),[36] [(($OMe)_2$bpb)-Ru(NO)(Resf)] (**9-Resf**),[35] [($Me_2$bQb)Ru(NO)(Resf)] (**10-Resf**),[36] [(($OMe)_2$bQb)Ru(NO)(Resf)] (**11-Resf**),[36] and [(($OMe)_2$IQ1)-Ru(NO)(Resf)] (**12-Resf**),[35] the Resf dye is attached trans to NO (Figure 10). Unbound Resf in its deprotonated form exhibits strong absorbance in the visible region when dissolved in DMF ($\lambda_{max}$ = 590 nm, $\varepsilon$ = 105000 $M^{-1}$ $cm^{-1}$). This band, arising from a highly favored $\pi \rightarrow \pi^*$ transition, appears at low energy because of extensive delocalization of the negative charge of the phenolato-O moiety over the dye's tricyclic ring system. Upon coordination, the dye absorption band is blue-shifted (from 590 to 500 nm) with a significant reduction in intensity (for example, in **8-Resf**, $\varepsilon$ = 11920 $M^{-1}$ $cm^{-1}$). This is not unexpected since a similar trend is observed when Resf becomes protonated (470 nm, $\varepsilon$ = 20000 $M^{-1}$ $cm^{-1}$).

In all dye−nitrosyl conjugates, the overlap of the photoband of the parent nitrosyls with the strong 500 nm Resf absorption band results in sensitization toward visible light. As changes in the equatorial ligand frames red-shift the photobands of the parent nitrosyls (more toward the 500 nm dye band), the extent of sensitization is increased due to overlap of the two transitions. Since alterations of the equatorial ligands also bring about enhancement in the $\varepsilon$ values of the photoband of the parent nitrosyls (as shown in Figure 8), considerable overlap (in some cases merging) of the two bands leads to excellent sensitization, as in the case with **11-Resf** and **12-Resf**. The enhanced visible light absorption provides considerably increased NO photolability with 500 nm light in such cases. For example, the photoband of **8** is at 395 nm and **8-Resf** has a quantum yield value of 0.052 at 500 nm, while the photoband of **12** is at 475 nm and **12-Resf** has a quantum yield value of 0.270 (Figure 11). However, when one compares **11-Resf** ($\phi_{500}$ = 0.206) and **12-Resf** ($\phi_{500}$ = 0.270), even though **11** has a $\lambda_{max}$ at 490 nm and **12** at 475 nm, the greater intensity of the photoband of **12** ($\varepsilon$ = 8700 $M^{-1}$ $cm^{-1}$) leads to more overlap with the dye band compared with **11** ($\varepsilon$ = 3750 $M^{-1}$ $cm^{-1}$). It is thus evident that the energy absorbed by the dye is transferred to the RuNO unit allowing enhanced photodissociation of NO under 500 nm light. The direct attachment of the sensitizing chromophore to the RuNO unit clearly affords greater extent of sensitization (Figure 9) compared with peripheral attachment of the chromophore via linkers.

In order to gain further insight into the mechanism of energy transfer between the dye molecule and the $\{RuNO\}^6$ core, DFT studies were preformed on **11-Resf**. Inspection of the energy and shape of the MOs of **11-Resf** reveals many similarities to those found on the ($OMe_2$bQb)Ru(NO) unit of **11**. However, in the case of **11-Resf**, MOs with Resf

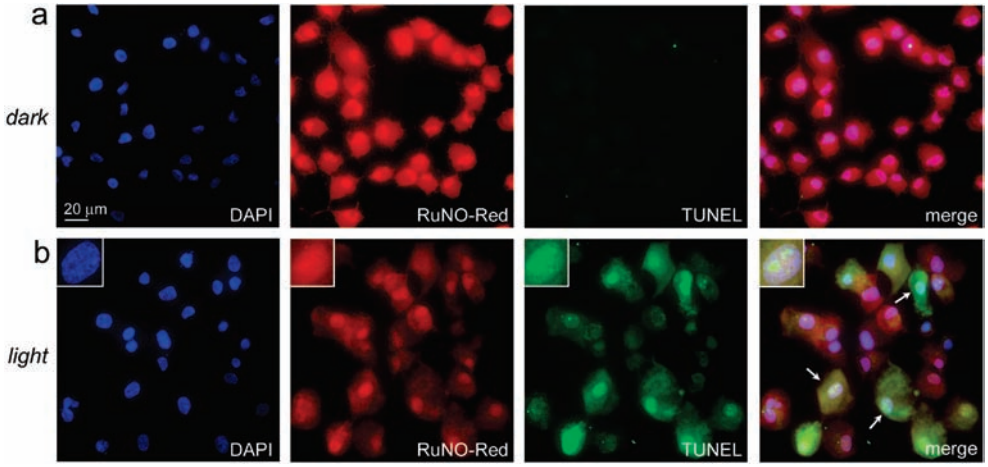


**FIGURE 13.** Fluorescence microscopy of apoptotic MDA-MB-231 cells treated with 200 $\mu$M **8-Resf** and either (a) kept in the dark or (b) exposed to 1 min visible light ($\lambda \geq 465$ nm, 0.3 W). Insets: magnified views of an apoptotic cell showing TUNEL-detected DNA fragmentation. [DAPI = 4′,6-diamidino-2-phenylindole; TUNEL = terminal dUPT nick end labeling].

character are interspersed throughout the MO manifold of the {$(OMe_2bQb)Ru(NO)$}. We were interested to see which of these orbitals were involved in the transition at 500 nm and thus preformed time-dependent DFT (TDDFT) studies.[40] The resulting calculated electron absorption spectrum of **11-Resf** exhibits a strong band at 500 nm similar to that observed in the experimental spectrum. This band has its origin in a transition from a combination of $\pi$(PDA)$-\pi$(RuNO) and a $\pi$(Resf) MO to the $\pi^*$(Resf)$\pi^*$(RuNO) MO in the LUMO manifold (Figure 12). These results confirm that direct attachment of the Resf chromophore allows for efficient through-bond energy transfer from the Resf to the RuNO moiety and provide an explanation for the enhanced NO photolability of the dye−nitrosyl conjugate.

With the direct attachment of Resf, we have been able to induce significant sensitivity of the {RuNO}$^6$ nitrosyls to 500 nm light. The question then arose whether attachment of other dyes with strong absorption at wavelength longer than 500 nm sensitizes the {RuNO}$^6$ unit to even lower energy light. In PDT, it is known that the addition of a heavy atom to a sensitizer increases the range as well as capacity of sensitization.[41] We therefore synthesized two iso-electronic heavy-atom analogues of Resf, namely, thionol (Thnl) and selenophore (Seln) via replacement of the ring O with S and Se, respectively.[40] As the size of the atoms increases from O to S to Se, there is a systematic shift in the $\lambda_{max}$ (590 to 610 to 612 nm) of the corresponding dyes. All three dyes were directly attached to the {$((OMe)_2bQb)Ru(NO)$} unit for a clear comparison of the extent of sensitization by each dye. As expected, both [$((OMe)_2bQb)Ru(NO)(Thnl)$] (**11-Thnl**) and [$((OMe)_2bQb)Ru(NO)(Seln)$] (**11-Seln**) display red-shifted dye bands (with $\lambda_{max}$ at 525 and 535 nm, respectively) compared with that of **11-Resf** (dye band at 500 nm). In addition, the dye bands in both **11-Thnl** and **11-Seln** are much broader, a fact that leads to greater photosensitivity over a larger range of wavelengths in the visible region. For example, **11-Resf** releases NO upon exposure to light $\leq$525 nm, while **11-Thnl** releases NO with light $\leq$550 nm. Finally, **11-Seln** releases NO with light $\leq$600 nm. This suggests that the "heavy-atom chromophore effect" is indeed playing a role in the photosensitization of these dye−nitrosyl conjugates. Collectively, these results now demonstrate that direct attachment of visible light-harvesting chromophores to {RuNO}$^6$ nitrosyls can impart excellent NO photolability under light in the visible range (500−600 nm). Such chromophores need not to be exclusively organic. For example, da Silva and co-workers have reported NO photorelease from the pyrazine-bridged ruthenium nitrosyl $[Ru(NH_3)_5(pz)Ru(bpy)_2(NO)](PF_6)_2$ (pz = pyrazine, bpy = bipyridine) upon irradiation at 532 nm.[42,43] In this instance, the $d_\pi Ru(II) \rightarrow \pi^*(pz)$ metal-to-ligand charge transfer (MLCT) transition of the {$Ru(NH_3)_5(pz)$} moiety at ~550 nm promotes the release of NO and thus acts as the light-harvesting unit.

## Utility of the Sensitized Ruthenium Nitrosyls

With the quest of new photoactive ruthenium nitrosyls still ongoing in this laboratory, mention must be made here regarding the utility of the nitrosyls that we have already synthesized. Since the present {RuNO}$^6$ nitrosyls rapidly release NO upon exposure to low-power visible light (450−600 nm), they could be readily employed as PDT agents to cause apoptosis of cellular targets. We have

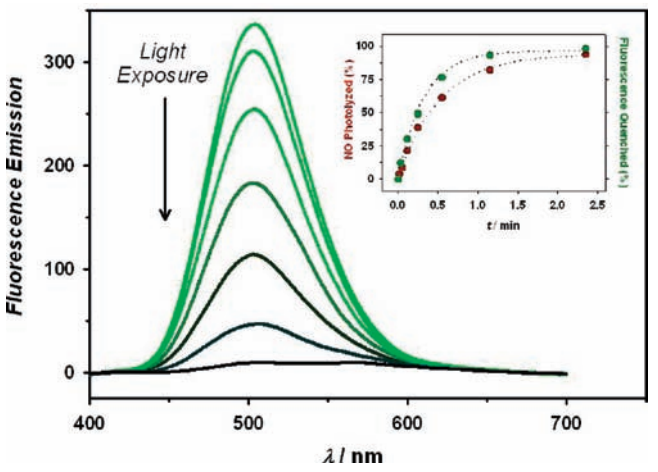


**FIGURE 14.** Fluorescence quenching observed upon photolysis of **8-Ds-Im** ($\lambda_{irr} \geq 400$ nm, 0.5 W) in aqueous phosphate buffer (pH 7.4). Inset: correlation between percent NO photorelease and percent fluorescence quenched during the same photolysis experiment.

already demonstrated that indeed one can promote NO-induced apoptosis in human breast cancer cells (MDA-MB-231) via light-triggered NO delivery from the dye-sensitized nitrosyl **8-Resf**.[36] These cells have previously been shown to undergo apoptosis in the presence of elevated NO concentrations.[44] Incidentally, the additional advantage of the red fluorescence of **8-Resf** (due to attached Resf dye) allows for visualization of the location of the NO donor within the cells in our experiments. Upon incubation, **8-Resf** is easily taken up by the living cells as evidenced by the red fluorescent nuclear staining patterns observed in Figure 13 (panel a). When left in the dark over the course of 8 h, these cells show no significant signs of death. However, if the nitrosyl-loaded cells are exposed to visible light ($\lambda \geq 465$ nm, 0.3 W) for only 1 min, they begin to show signs of apoptosis after 4−8 h (Figure 13, panel b). This time frame is similar to that observed in similar studies for NO-induced apoptosis. Images of the light exposed cells show chromatin condensation and fragmentation (as evidenced by TUNEL assay, Figure 13, panel b) and breakdown of cellular walls indicating apoptosis. In control experiments, nitrosyl-free cells under similar conditions (in the dark and under light) remain unharmed and thus confirm that simple light exposure is not the cause of cell death.

Another added bonus of these dye-sensitized nitrosyls is the fact that these NO donors come with a fluorometric on/off switch. The initial fluorescence of the dye-tethered $\{RuNO\}^6$ nitrosyls (as shown in Figure 13 for **8-Resf**) is quenched following photorelease of NO since the photoproducts are paramagnetic low-spin Ru(III) species of the type $[(L)Ru(solv)(dye)]^{n+}$ (where L = designed ligand, solv = solvent).[36] As a consequence, such NO donors are "trackable" in cellular experiments. One can follow the entrance of the NO donor in the cell from its initial fluorescence and once the NO delivery is over, the fluorescence is turned off. In a separate experiment, we have employed the designed nitrosyl $[(Me_2bpb)Ru(NO)(Ds\text{-}Im)](BF_4)$ (**8-Ds-Im**, Ds-Im = dansyl imidazole[45]) with a dansyl fluorophore to test this hypothesis of "trackable NO donors".[46] The kinetics of light-induced NO release and the loss of green fluorescence of this NO donor correlate very closely (Figure 14). When added to MDA-MB-231 cells, the cells exhibit strong green fluorescence. Upon exposure to visible light for 1 min, the green fluorescence is turned off due to NO release within the cells and eventually apoptosis sets in.

## Closing Remarks

Although the stability and NO photolability of $\{RuNO\}^6$ nitrosyls were known for quite some time, their use in NO-induced PDT has been quite restricted because of their sensitivity to UV light. Research in our laboratory has now delineated new strategies of sensitization of ruthenium nitrosyls. The designed $\{RuNO\}^6$ nitrosyls readily release NO upon exposure to low-power visible light, which thus makes them suitable for PDT use. Our work has also demonstrated that cellular apoptosis can be induced by these nitrosyls under the control of visible light. We have also incorporated selected nitrosyls in polymer matrices[47,48] and used patches of such materials to deliver NO to biological targets.[49,50] Such patches could find use in combating skin infections and malignancies via delivery of NO to selected areas under the control of light. Clearly, there are many uses of ruthenium NO donors that are sensitive to visible/near-IR light and research toward further development in this area will be both exciting and rewarding.

*Financial support from the NSF Grants CHE-0553405 and CHE-0957251 is gratefully acknowledged.*

BIOGRAPHICAL INFORMATION

**Nicole L. Fry** was born in Auburn, CA, in 1983. She received her B. S. in chemistry from Sonoma State University in 2006. Since then, she has been working as a graduate student in the research group of Professor Pradip Mascharak in the Department of Chemistry and Biochemistry at the University of California, Santa Cruz. Her research interests include the design and syntheses of photoactive ruthenium nitrosyls and their utility as NO donors to cellular targets.

**Pradip K. Mascharak** was born in Jaipur, India, in 1953. He received his Ph.D. from the Indian Institute of Technology, Kanpur, in 1979. In the same year, he joined the research group of Professor Richard Holm at Stanford University and later moved to Harvard University. He later worked with Professor Steve Lippard at the Massachusetts Institute of Technology for two years before joining the University of California, Santa Cruz (UCSC), in late 1984. He is currently a Professor of Chemistry and Biochemistry at UCSC. Modeling the active sites of metalloenzymes, design of complexes that exhibit oxygenase activity in the presence of peroxides and dioxygen, and syntheses of photoactive NO donors are the major focus of his research.

## FOOTNOTES

*To whom correspondence should be addressed. E-mail: pradip@chemistry.ucsc.edu.

## REFERENCES


1 *Nitric Oxide: Biology and Pathobiology*; Ignarro, L. J., Ed.; Academic Press: San Diego, CA, 2000.

2 Kalsner, S. *Nitric Oxide and Free Radicals in Peripheral Neurotransmission*; Birkhäuser: Boston, MA, 2000.

3 *Nitric Oxide and Infection*; Fang, F. C., Ed.; Kluwer Academic/Plenum Publishers: New York, 1999.

4 *Nitric Oxide and Cell: Proliferation, Differtiation and Death*. Moncada, S., Higgs, E. A., Bagetta, G., Eds.; Portland Press: London, 1998.

5 Degoute, C. S. Controlled Hypotension — A Guide to Drug Choice. *Drugs* **2007**, *67*, 1053–1076.

6 Hetrick, E. M.; Schoenfisch, M. H. Reducing Implant-Related Infections: Active Release Strategies. *Chem. Soc. Rev.* **2006**, *35*, 780–789.

7 Frost, M. C.; Reynolds, M. M.; Meyerhoff, M. E. Polymers Incorporating Nitric Oxide Releasing/Generating Subtances for Improved Biocompatibility of Blood-Contacting Devices. *Biomaterials* **2005**, *26*, 1685–1693.

8 Fang, F. C. Antimicrobial Reactive Oxygen and Nitrogen Species: Concepts and Controversies. *Nat. Rev. Microbiol.* **2004**, *2*, 820–832.

9 Fang, F. C. Mechanisms of Nitric Oxide-Related Antimicrobial Activity. *J. Clin. Invest.* **1997**, *99*, 2818–2825.

10 Kanwar, J. R.; Kanwar, R. K.; Burrow, H.; Baratchi, S. Recent Advances on the Role of NO in Cancer and Chronic Inflammatory Disorders. *Curr. Med. Chem.* **2009**, *16*, 2373–2394.

11 Hirst, D.; Robson, T. Targeting Nitric Oxide for Cancer Therapy. *J. Pharm. Pharmacol.* **2007**, *59*, 3–13.

12 Xu, W.; Liu, L. Z.; Loizidou, M.; Ahmed, M.; Charles, I. G. The Role of Nitric Oxide in Cancer. *Cell Res.* **2002**, *12*, 311–320.

13 Wang, P. G.; Cai, T. B.; Taniguchi, N. *Nitric Oxide Donors for Pharmaceutical and Biological Applications*; Wiley-VCH: Weinheim, Germany, 2005.

14 Eroy-Reveles, A. A.; Mascharak, P. K. Nitric Oxide-Donating Materials and Their Potential in Phamacological Applications for Site-Specific Nitric Oxide Delivery. *Future Med. Chem.* **2009**, *8*, 1497–1507.

15 Rose, M. J.; Mascharak, P. K. Fiat Lux: Selective Delivery of High Flux of Nitric Oxide (NO) to Biological Targets Using Photoactive Metal Nitrosyls. *Curr. Opin. Chem. Biol.* **2008**, *12*, 238–244.

16 Rose, M. J.; Mascharak, P. K. Photoactive Ruthenium Nitrosyls: Effects of Light and Potential Application as NO Donors. *Coord. Chem. Rev.* **2008**, *252*, 2093–2114.

17 Ostrowski, A. D.; Ford, P. C. Metal Complexes as Photochemical Nitric Oxide Precursors: Potential Applications in the Treatment of Tumors. *Dalton Trans.* **2009**, 10660–10669.

18 Levina, A.; Mitra, A.; Lay, P. A. Recent Developments in Ruthenium Anticancer Drugs. *Metallomics* **2009**, *1*, 458–470.

19 Cox, A. B.; Wallace, R. N. Photolysis of Nitrosylruthenium Chloro Complexes. *Inorg. Nucl. Chem. Lett.* **1971**, *7*, 1191–1194.

20 Tfouni, E.; Krieger, M.; McGarvey, B. R.; Franco, D. W. Structure, Chemical and Photochemical Reactivity and Biological Activity of Some Ruthenium Amine Nitrosyl Complexes. *Coord. Chem. Rev.* **2003**, *236*, 57–69.

21 Tfouni, E.; Doro, G.; Figueiredo, E.; Pereira, C. M.; Metzke, G.; Franco, D. W.; Tailoring, N. O. Donors Metallopharmaceuticals: Ruthenium Nitrosyl Ammines and Aliphatic Tetraazamacrocycles. *Curr. Med. Chem.* **2010**, *17*, 3643–3657.

22 Bigio, I. J.; Bown, S. G. Spectroscopic Sensing of Cancer and Cancer Therapy- Current Status of Translational Research. *Cancer Biol. Ther.* **2004**, *3*, 259–267.

23 Dolmans, D. E. J. G.; Fukumura, D.; Jain, R. K. Photodynamic Therapy for Cancer. *Nat. Rev. Cancer* **2003**, *3*, 380–387.

24 Ghosh, K.; Eroy-Reveles, A. A.; Holman, T. R.; Olmstead, M. M.; Mascharak, P. K. Reactions of NO with Mn(II) and Mn(III) Center Coordinated to Carboxamido Nitrogen: Synthesis of a Manganese Nitrosyl with Photolabile NO. *Inorg. Chem.* **2004**, *43*, 2988–2997.

25 Hoffman-Luca, C. G.; Eroy-Reveles, A. A.; Alvarenga, J.; Mascharak, P. K. Syntheses, Structures, and Photochemistry of Manganese Nitrosyls Derived from Designed Schiff Base Ligands: Potential NO Donors That can be Activated by Near-Infrared Light. *Inorg. Chem.* **2009**, *48*, 9104–9111.

26 Patra, A. K.; Rowland, J. M.; Marlin, D. S.; Bill, E.; Olmstead, M. M.; Mascharak, P. K. Iron Nitrosyls of a Pentadentate Ligand Containing a Single Carboxamide group: Syntheses, Structures, Electronic properties and Photolability of NO. *Inorg. Chem.* **2003**, *42*, 6812–6823.

27 Patra, A. K.; Afshar, R. K.; Olmstead, M. M.; Mascharak, P. K. The First Non-Heme Iron(III) Complex with a Carboxamido Group That Exhibits Photolability of a Bound NO Ligand. *Angew. Chem., Int. Ed.* **2002**, *41*, 2512–2515.

28 Patra, A. K.; Mascharak, P. K. A Ruthenium Nitrosyl That Rapidly Delivers NO to Proteins in Aqueous Solution upon Short Exposure to UV Light. *Inorg. Chem.* **2003**, *42*, 7363–7365.

29 The $\{MNO\}^n$ notation used in this article is that of Feltham and Enemark. See: Enemark, J; Feltham, R. D. *Coord. Chem. Rev.* **1974**, *13*, 339–406.

30 Szundi, I.; Rose, M. J.; Sen, I.; Eroy-Reveles, A. A.; Mascharak, P. K.; Einarsdottir, O. A New Approach for Studying Fast Biological Reactions Involving Nitric Oxide: Generation of NO Using Photolabile Ruthenium and Manganese NO Donors. *Photochem. Photobiol.* **2006**, *82*, 1377–1384.

31 Madhani, M.; Patra, A. K.; Miller, T. W.; Eroy-Reveles, A. A.; Hobbs, A. J.; Fukuto, J. M.; Mascharak, P. K. Biological Activity of Designed Photolabile Metal Nitrosyls: Light-Dependent Activation of Soluble Guanylate Cyclase and Vasorelaxant Properites in Rat Aorta. *J. Med. Chem.* **2006**, *49*, 7325–7330.

32 Rose, M. J.; Patra, A. K.; Alcid, E. A.; Olmstead, M. M.; Mascharak, P. K. Ruthenium Nitrosyls Derived from Polypyridine Ligands with Carboxamide or Imine Nitrogen Donor(s): Isoelectronic Complexes with Different NO Photolability. *Inorg. Chem.* **2007**, *46*, 2328–2338.

33 Fry, N. L.; Rose, M. J.; Rogow, D. L.; Nyitray, C.; Kaur, M.; Mascharak, P. K. Ruthenium Nitrosyls Derived from Tetradentate Ligands Containing Carboxamido-N and Phenolato-O Donors: Syntheses, Structures, Photolability, and Time Dependent Density Functional Theory Studies. *Inorg. Chem.* **2010**, *49*, 1487–1495.

34 Patra, A. K.; Rose, M. J.; Murphy, K. M.; Olmstead, M. M.; Mascharak, P. K. Photolabile Ruthenium Nitrosyls with Planar Dicarboxamide Tetradentate N4 Ligands: Effects of In-Plane and Axial Ligand Strength on NO Release. *Inorg. Chem.* **2004**, *43*, 4487–4495.

35 Fry, N. L.; Heilman, B. J.; Mascharak, P. K. Dye-Tethered Ruthenium Nitrosyls Containing Planar Dicarboxamide Tetradentate N4 Ligands: Effects of In-Plane Ligand Twist on NO Photolability. *Inorg. Chem.* **2011**, *50*, 317–324.

36 Rose, M. J.; Fry, N. L.; Marlow, R.; Hink, L.; Mascharak, P. K. Sensitization of Ruthenium Nitrosyls to Visible Light via Direct Coordination of the Dye Resorufin: Trackable NO Donors for Light-Triggered NO Delivery to Cellular Targets. *J. Am. Chem. Soc.* **2008**, *130*, 8834–8846.

37 Rose, M. J.; Olmstead, M. M.; Mascharak, P. K. Photosensitization via Dye Coordination: A New Strategy to Synthesize Metal Nitrosyls That Release NO Under Visible Light. *J. Am. Chem. Soc.* **2007**, *129*, 5342–5343.

38 Wecksler, S. R.; Hutchinson, J.; Ford, P. C. Toward Development of Water Soluble Dye Derivatized Nitrosyl Compounds for Photochemical Delivery of NO. *Inorg. Chem.* **2006**, *45*, 1192–1200.

39 Conrado, C. L.; Wecksler, S.; Egler, C.; Magde, D.; Ford, P. C. Synthesis and Photochemical Properties of a Novel Iron-Sulfur-Nitrosyl Cluster Derivatized with the Pendant Chromophore Protoporphyrin IX. *Inorg. Chem.* **2004**, *43*, 5543–5549.

40 Rose, M. J.; Mascharak, P. K. Photosensitization of Ruthenium Nitrosyls to Red Light with an Isoelectronic Series of Heavy-Atom Chromophores: Experimental and Density Functionalz Theory Studies on the Effects of O-, S- and Se-Substituted Coordinated Dyes. *Inorg. Chem.* **2009**, *48*, 6904–6917.

41 Koziar, J. C.; Cowan, D. O. Photochemical Heavy-Atom Effects. *Acc. Chem. Res.* **1978**, *11*, 334–341.

42 Sauaia, M. G.; de Lima, R. G.; Tedesco, A. C.; da Silva, R. S. Photoinduced NO Release by Visible Light Irradiation from Pyrazine-Bridged Nitrosyl Ruthenium Complexes. *J. Am. Chem. Soc.* **2003**, *125*, 14718–14719.

43 Sauaia, M. G.; de Lima, R. G.; Tedesco, A. C.; da Silva, R. S. Nitric Oxide Production by Visible Light Irradiation of Awqueos Solution of Nitrosyl Ruthenium Complexes. *Inorg. Chem.* **2005**, *44*, 9946–9951.

44 Simeone, A. M.; Colella, S.; Krahe, R.; Johnson, M. M.; Mora, E.; Tari, A. M. N-(4-Hydroxyphenyl)retinamide and Nitric Oxide Pro-drugs Exhibit Apoptotic and Anti-invasive Effects against Bone Metastatic Breast Cancer Cells. *Carcinogenesis* **2006**, *27*, 568–577.

45 Hilderbrand, S. A.; Lim, M. H.; Lippard, S. J. Dirhodium Tetracarboxylate Scaffolds as Reversible Fluorescence-Based Nitric Oxide Sensors. *J. Am. Chem. Soc.* **2004**, *126*, 4972–4978.

46 Rose, M. J.; Mascharak, P. K. A Photosensitive $\{Ru-NO\}^6$ Nitrosyl Bearing Dansyl Chromophore: Novel NO Donor with a Fluorometric On/Off Switch. *Chem. Commun.* **2008**, *33*, 3933–3935.

47 Eroy-Reveles, A. A.; Leung, Y.; Beavers, C. M.; Olmstead, M. M.; Mascharak, P. K. Near-Infrared Light Activated Release of Nitric Oxide from Designed Photoactive Manganese Nitrosyls: Strategy, Design, and Potential as NO Donors. *J. Am. Chem. Soc.* **2008**, *130*, 4447–4458.

48 Halpenny, G. M.; Olmstead, M. M.; Mascharak, P. K. Incorporation of a Designed Ruthenium Nitrosyl in PolyHEMA Hydrogel and Light-Activated Delivery of NO to Myoglobin. *Inorg. Chem.* **2007**, *46*, 6601–6606.

49 Halpenny, G. M.; Steinhardt, R. C.; Okialda, K. A.; Mascharak, P. K. Characterization of pHEMA-Based Hydrogels That Exhibit Light-Induced Bactericidal Effect via Release of NO. *J. Mater Sci: Mater. Med.* **2009**, *20*, 2353–2360.

50 Halpenny, G. M.; Gandhi, K. R.; Mascharak, P. K. Eradication of Pathogenic Bacteria by Remote Delivery of NO via Light Triggering of Nitrosyl-Containing Materials. *ACS Med. Chem. Lett.* **2010**, *1*, 180–183.